Available online at www.sciencedirect.com

SCIENCE DIRECT®

ELSEVIER

Journal of Computational and Applied Mathematics 168 (2004) 437–446

JOURNAL OF COMPUTATIONAL AND APPLIED MATHEMATICS

www.elsevier.com/locate/cam

Magnetic field computation for optimized shielding of induction heaters

P. Sergeant*, L. Dupré, J. Melkebeek, L. Vandenbossche

Department of Electrical Energy, Systems and Automation, Ghent University, Sint-Pietersnieuwstraat 41, Gent B-9000, Belgium

Received 5 August 2002; received in revised form 5 August 2003

Abstract

We consider a finite element model for passive and active shielding of the magnetic stray field of induction heaters. In induction heaters, a metallic workpiece is heated by induced eddy currents. These currents are caused by a strong alternating magnetic field, generated by the excitation coil that surrounds the workpiece. First, an axisymmetric, quasi-static and time-harmonic numerical model of the induction heater is developed. The electrical currents are azimuthal. Next, passive shields are added, using impedance boundary conditions, relating the tangential components of the electric field E and the magnetic field H at the surface of the passive shield. Additionally, the possibility of active shielding is deepened. A number of extra coils is added to the finite element model. The currents in these compensation coils should generate counter fields. The best position and currents in the compensation coils are identified from a proper inverse problem.

MSC: 02.70.Dh; 02.60.Lj; 41.20.Gz

Keywords: Induction heater; Magnetic field; Passive shield; Active shield

1. Introduction

Induction heater equipment is exploited for a thermal treatment of metallic specimen. This thermal treatment is obtained by huge eddy currents, induced in the conductive specimen. The eddy currents result from the time dependent magnetic field, generated by the excitation coil.

The magnetic field generated by the excitation coil is extended in the whole surrounding region. This gives rise to magnetic field levels that may be significantly higher than the ICNIRP reference

* Corresponding author.
E-mail address: peter.sergeant@rug.ac.be (P. Sergeant).

0377-0427/$ - see front matter
doi:10.1016/j.cam.2003.12.006

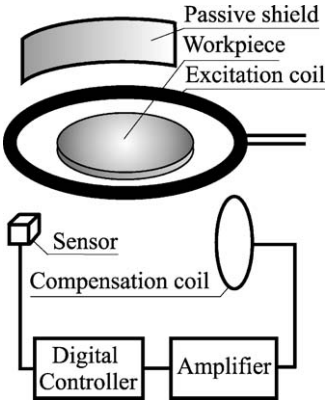

Fig. 1. Principle of active and passive shielding.

levels [3]. The operator controlling the heating process and electronic devices in the neighbourhood are exposed to the field, as they work in close proximity of the equipment. Therefore, the magnetic fields should be mitigated using three techniques:

- reconsideration of the induction heater design,
- passive shielding, using suitable materials to limit electromagnetic losses within the shield [5],
- active shields, generating counter fields opposite to the main one to be reduced. A number of coils has to be added at well-chosen positions, taking into account the accessibility of the workpiece. Eventually, a control system using the signals of B-field sensors can be developed [1] as shown in Fig. 1. Consequently, the effectiveness of the active shield is guaranteed in case of changing fields due to thermal effects, proximity of conductive and/or magnetic apparatus, and changing geometries.

The modification of the thermal treatment of the workpiece by the reduction of the magnetic environmental pollution, must be limited to a minimum.

2. Numerical model for the environment of the induction heater

The modelled induction heater consists of an excitation coil of 20 cm radius and a 1 cm thick aluminium disc with a radius of 19 cm. Fig. 2 illustrates the geometry. The linear model is quasi-static and time-harmonic.

The domain Ω is defined by the disc, the excitation and compensation coils and the air surrounding the induction heater. In the numerical field calculation, the known current density in these coils is denoted by $\bar{J}_e = J_e(r,z)\bar{1}_\phi$. The regions of the conducting passive shields are excluded. In the domain Ω, the magnetic induction is written as $\bar{B} = \bar{\nabla} \times \bar{A}$, with the vector potential $\bar{A} = A_\phi(r,z)\bar{1}_\phi$. It is well known from Maxwell equations that $A_\phi(r,z)$ obeys a second-order boundary value problem (BVP)

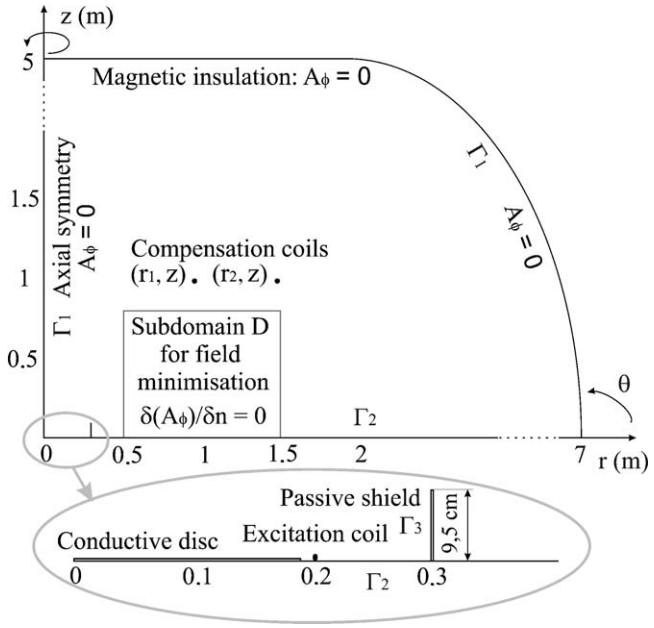

Fig. 2. Finite-element lay-out, scales in metre (FEM: magnetic vector potential $\bar{A} = A_\phi \bar{1}_\phi$).

in Ω, i.e.,

$$\left(\frac{\partial}{\partial r}\left(\frac{1}{r\mu}\frac{\partial}{\partial r}(rA_\phi)\right)\right) + \left(\frac{\partial}{\partial z}\left(\frac{1}{r\mu}\frac{\partial}{\partial z}(rA_\phi)\right)\right) - j\sigma\omega A_\phi = -J_e \tag{1}$$

together with the boundary conditions (BCs), see Fig. 2,

$$A_\phi = 0 \text{ on } \Gamma_1, \tag{2}$$

$$\left(\frac{1}{r}\frac{\partial}{\partial r}(rA_\phi).n_r + \frac{1}{r}\frac{\partial}{\partial z}(rA_\phi).n_z\right) = 0 \text{ on } \Gamma_2, \tag{3}$$

$$\left(\frac{1}{r}\frac{\partial}{\partial r}(rA_\phi).n_r + \frac{1}{r}\frac{\partial}{\partial z}(rA_\phi).n_z\right) = jA_\phi e^{-j\pi/4}\sqrt{\sigma_p\omega\mu_p} \text{ on } \Gamma_3. \tag{4}$$

Here μ and σ are the permeability and the electric conductivity of the material present in Ω while μ_p and σ_p are the values for the passive shield. $f = \omega/2\pi$ is the frequency of the source term J_e. The BC on Γ_1 describes magnetic isolation while the homogeneous BC on Γ_2 forces the flux lines to be normal to the symmetry line $z = 0$. The BC on Γ_3 is based on the notion that for small skin depths electromagnetic fields penetrate locally and consequently that at each boundary point, tangential components of electric and magnetic fields are related to one another almost in the same way as in the case of a plane wave penetrating a conducting half space. The impedance BC (IBC) on Γ_3 describes the relation between these two tangential components in the case of a linear magnetic material of the passive shield [4].

In order to solve this BVP we use a finite element approximation. We construct a finite dimensional subspace X_h of $H^1(\Omega)$ using the partition τ_h of $\bar{\Omega}$ in triangles. We take $X_h = \{v \in C^0(\bar{\Omega}); v$ is a linear

function in each element $K \in \tau_h\}$. Let $[r_i, z_i]$, $1 \leqslant i \leqslant N$, be the set of all nodes, i.e., the set of all vertices of all triangles $K \in \tau_h$. The cardinal basis functions of X_h, defined by $\varphi_i(r_j, z_j) = \delta_{ij}$ for i and $j = 1, \ldots, N$, are used as the set of interpolation functions in the FE scheme.

A 1 m long and 0.8 m high rectangle in Fig. 2 symbolises the subdomain D where the operator is working and where the average magnetic induction B should be minimized. A strongly refined finite element mesh to evaluate the electromagnetic fields inside the passive shield is avoided by introducing the BC (4). A number of compensation coils can be found in Fig. 2. Together with the passive shield, they should minimise B in subdomain D.

3. Design of the active shield

3.1. Method

To reduce the stray field in the subdomain D, the positions of the compensation coils and the currents in the coils must be identified from a proper inverse problem. The optimal position of the coils is found iteratively [2]. During each iteration—with fixed position—, the currents in the compensation coils are optimized by the least squares method, which minimises the average of the B-field norms in several points in subdomain D.

3.2. The least squares method to find the currents (fixed coil positions)

In the model, N compensation coils are considered. In a time-harmonic calculation, $\bar{B} = B_r \bar{1}_r + B_z \bar{1}_z$ consists in each point of two complex components $B_r = B_{r,r} + \mathrm{i}B_{r,i}$ and $B_z = B_{z,r} + \mathrm{i}B_{z,i}$. Similarly, the current $I_k \bar{1}_\phi$ in coil k has a real and imaginary component: $I_k = I_{r,k} + \mathrm{i}I_{i,k}$. When the compensation coil k carries $I_{r,k} = 1A$ current and with zero current in all other coils, the r- and z-components of $\bar{B}$ are denoted by $b_{r,r,k}$, $b_{r,i,k}$, $b_{z,r,k}$, and $b_{z,i,k}$. The total induction, generated by the excitation coil and N compensation coils, is

$$
\begin{aligned}
B_{r,r} &= B_{r,r,e} + \sum_{k=1}^{N} (b_{r,r,k} I_{r,k} - b_{r,i,k} I_{i,k}), \\
B_{r,i} &= B_{r,i,e} + \sum_{k=1}^{N} (b_{r,i,k} I_{r,k} + b_{r,r,k} I_{i,k}), \\
B_{z,r} &= B_{z,r,e} + \sum_{k=1}^{N} (b_{z,r,k} I_{r,k} - b_{z,i,k} I_{i,k}), \\
B_{z,i} &= B_{z,i,e} + \sum_{k=1}^{N} (b_{z,i,k} I_{r,k} + b_{z,r,k} I_{i,k})
\end{aligned} \tag{5}
$$

with $B_{r,r,e}$, $B_{r,i,e}$, $B_{z,r,e}$ and $B_{z,i,e}$ the real and imaginary r- and z- contribution of the excitation current. The norm of the induction B is the square root of

$$
B^2 = B_{r,r}^2 + B_{r,i}^2 + B_{z,r}^2 + B_{z,i}^2. \tag{6}
$$

The matrix A is constructed from the partial derivatives of B^2 to the currents $I_{r,k}$ and $I_{i,k}$:

$$A = \begin{bmatrix} \dfrac{\partial B^2}{\partial I_{r,1}^2} & \dfrac{\partial B^2}{\partial I_{r,1}\partial I_{i,1}} & \dfrac{\partial B^2}{\partial I_{r,1}\partial I_{r,2}} & \cdots & \dfrac{\partial B^2}{\partial I_{r,1}\partial I_{i,N}} \\ \dfrac{\partial B^2}{\partial I_{i,1}\partial I_{r,1}} & \dfrac{\partial B^2}{\partial I_{i,1}^2} & \dfrac{\partial B^2}{\partial I_{i,1}\partial I_{r,2}} & \cdots & \dfrac{\partial B^2}{\partial I_{i,1}\partial I_{i,N}} \\ \dfrac{\partial B^2}{\partial I_{r,2}\partial I_{r,1}} & \dfrac{\partial B^2}{\partial I_{r,2}\partial I_{i,1}} & \dfrac{\partial B^2}{\partial I_{r,2}\partial I_{r,2}} & \cdots & \dfrac{\partial B^2}{\partial I_{r,2}\partial I_{i,N}} \\ \vdots & \vdots & \vdots & \ddots & \vdots \\ \dfrac{\partial B^2}{\partial I_{i,N}\partial I_{r,1}} & \dfrac{\partial B^2}{\partial I_{i,N}\partial I_{i,1}} & \dfrac{\partial B^2}{\partial I_{i,N}\partial I_{r,2}} & \cdots & \dfrac{\partial B^2}{\partial I_{i,N}^2} \end{bmatrix}, \tag{7}$$

while

$$C \text{ is } \begin{bmatrix} \dfrac{\partial B^2}{\partial I_{r,1}} & \dfrac{\partial B^2}{\partial I_{i,1}} & \dfrac{\partial B^2}{\partial I_{r,2}} & \cdots & \dfrac{\partial B^2}{\partial I_{i,N}} \end{bmatrix}^{\mathrm{T}}$$

with $I_{r,1} = I_{i,1} = I_{r,2} = \cdots = I_{i,N} = 0$.

In the subdomain D, a proper grid is chosen. In every node, the matrix A and C are calculated. Finally, all matrices are summed over the M points in the grid and the following linear equation is solved:

$$\left(\sum_{k=1}^{M} A\right) I = -\sum_{k=1}^{M} C, \tag{8}$$

wherein $I = [I_{r,1}, I_{i,1} I_{r,2} \cdots I_{i,N}]^{\mathrm{T}}$. I is the vector with the optimal currents in the N compensations coils, for fixed coil positions and excitation current.

3.3. Optimisation method to derive the positions

The optimization of the positions of the compensation coils is a problem of optimal control: a proper cost function has to be minimised, taking into account some constraints.

The cost function contains two terms. The first term is the integral over subdomain D of B^2, defined in (6). Its value is small in case of a low average B-norm in the subdomain. The second term equals $\sum_{k=1}^{N} R(I_{r,k}^2 + I_{i,k}^2)$, in order to penalise high installation and exploitation costs of the active shield. R is a weighting factor. Moreover, high compensation currents may affect the heating process in the workpiece.

To limit the number of variables, and to make the active shield realisable in practice, only nine compensation coils have been added to the model. The 18 variables (r_k and z_k, $k = 1, \ldots, 9$) are constrained as not all coil positions are convenient, due to the needed accessibility of the specimen.

4. Simulation results

4.1. No active nor passive shield

In the simulation, a sinusoidal excitation current of 4 kA at 1 kHz is used to heat a disc with a radius of 19 cm. Without any passive or active shield, the magnetic induction norm and its direction in the relevant part of the domain Ω are shown in Fig. 3. The average value of B in the subdomain is 26.1 μT, as shown in Table 1. The maximum value of 174 μT is found in the lower left corner of D. The energy dissipation in the workpiece W_{wp} is determined by integrating the energy dissipation of the induced eddy currents over the volume of the disc

$$W_{\mathrm{wp}} = 2\pi \int_S \frac{J^2}{\sigma} r \,\mathrm{d}r \,\mathrm{d}z \quad \text{with } J = -\mathrm{j}\sigma\omega A_\phi. \tag{9}$$

With 4000 A current in the one turn-excitation coil, W_{wp} is 1.133 kW. When adding shields, the change of W_{wp} should be limited to keep the heating process unaltered.

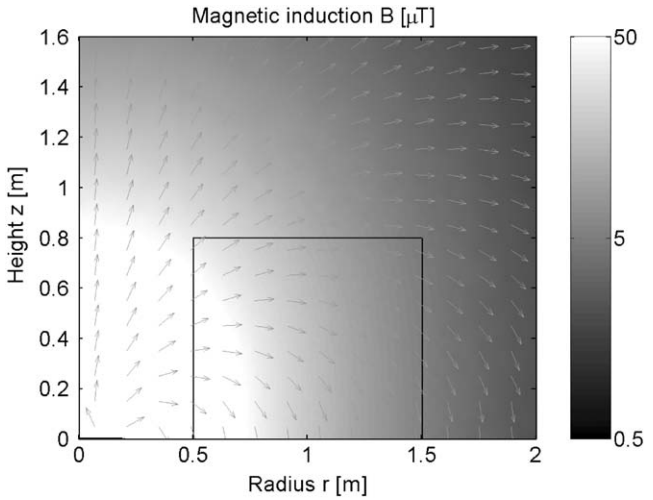

Fig. 3. Magnetic induction in case no shields are implemented.

Table 1
B in the subdomain D, induced heating in the workpiece W_{wp} and in the shield W_{p}

Shields	B_{avg} (μT)	B_{max} (μT)	W_{wp} (W)	W_{p} (W)
None	26.1	174	1133	—
Passive	8.80	48.9	1094	108
Pas. + act.; 9 indep. curr.	1.34	19.7	1097	110
Pas. + act.; 1 indep. curr.	2.18	23.0	1094	108

4.2. Passive shield

Especially in the lower left corner of subdomain D, the magnetic induction without any shields is high. Active field reduction in this part of subdomain D requires very high compensation currents, as the compensation coils are further away of this area than the excitation coil. A small passive shield causes here a significant field reduction so that it makes the active shield more efficient.

A passive shield with 19 cm height, 0.65 mm thickness and $\sigma_p = 5.9 \cdot 10^6/\Omega m$ is added to the model at 30 cm radius. With the shield, the model is not linear any more in the excitation and compensation currents, because the permeability μ_p of the shield depends slightly on the magnetic field H. However, as the amplitude of the excitation current is constant and the small compensation currents hardly influence the magnetic field around the shield, we can linearize the model by assuming μ_p constant. At the present induction level, μ_p of the shield was experimentally determined to equal 372 μ_0.

The BCs (4) can be used to model the passive shield in case that the skin depth δ is much smaller than half the shield thickness D_p. This implies

$$\delta = \sqrt{\frac{2}{\omega \sigma_p \mu_p}} << D_p \text{ or } D_{red} >> 1, \tag{10}$$

wherein $D_{red} = D_p/\delta$ is the reduced shield thickness. For low frequencies, the skin depth will be too high and a FE discretisation of the passive shield must be added to the numerical model as an alternative to IBC (4). With the shield thickness $D_p = 0.65$ mm, $\sigma_p = 5.9 \cdot 10^6/\Omega m$ and $\mu_p = 372\ \mu_0$, we find $D_{red} = 1.9$ for 1 kHz and $D_{red} = 6.1$ for 10 kHz. Fig. 5 shows that at 1 kHz, the use of the boundary conditions is not allowed, while at 10 kHz, both methods result in the same curve. The difference between FE and IBC modelling of the passive shield is then less than 1% if $D_{red} > 6$. For the calculations at 1 kHz in Fig. 4, a FE model of the passive shield has been

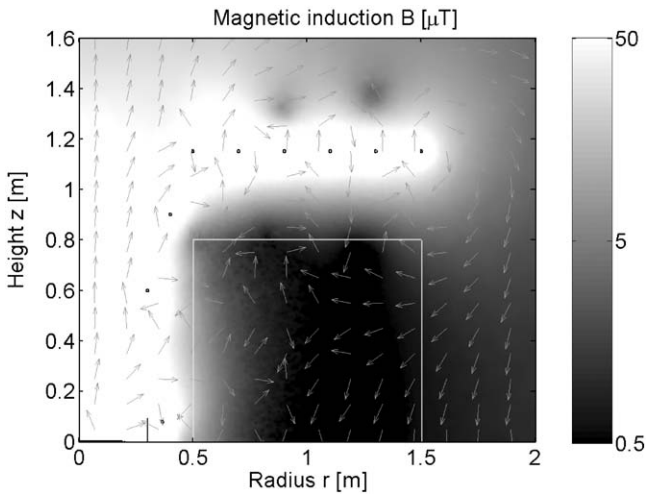

Fig. 4. Magnetic induction in case of passive and active shield.

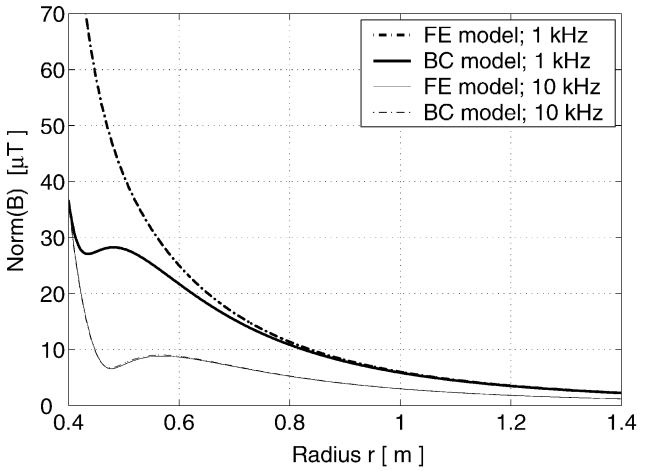

Fig. 5. Comparison of FE and BC models for the passive shield: $|B|$ at $z = 0$.

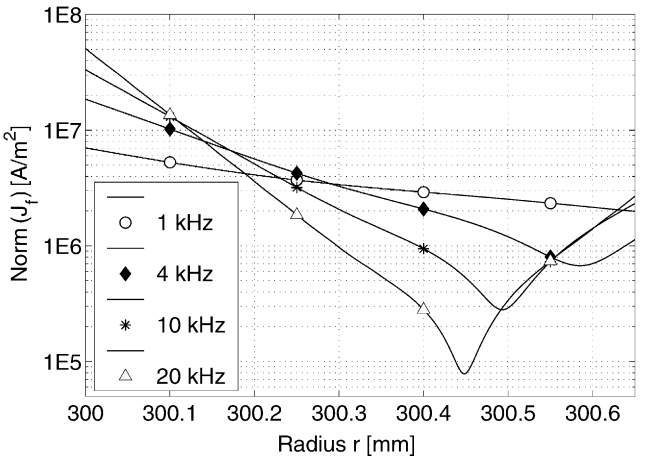

Fig. 6. Induced current density in the passive shield: $|J_f|$ at $z = 0$.

used. To guarantee the minimum D_{red}, it is allowed and even recommended to use IBC only for frequencies higher than 10 kHz.

The reason for the need of small skin depths is the fact that one side of the shield may not influence the other side. Fig. 6 visualizes the norm of the eddy currents in the shield for several frequencies. The minimum current density inside the shield is obviously lower for higher frequencies.

4.3. Passive and active shield with nine independent currents

Nine active compensation coils with positions displayed in Table 2 were added to the model as shown in Fig. 4. The positions are obtained from the procedure described in Section 3. From

Table 2
Coil positions obtained after optimisation; real and imaginary part of compensation currents in case of nine independent currents in one-turn coils; numbers of turns in case of one compensation current

Coil	1	2	3	4	5	6	7	8	9
r-co [m]	0.30	0.40	0.50	0.70	0.90	1.10	1.30	1.50	0.365
z-co [m]	0.60	0.90	1.15	1.15	1.15	1.15	1.15	1.15	0.08
Re(I_{opt}) [A]	82.3	45.0	−39.2	61.0	−37.3	36.5	−29.5	19.5	−5.03
Im(I_{opt}) [A]	19.3	−4.37	24.7	−14.7	6.1	−1.06	−1.20	1.57	66.6
Turns	8	4	−4	6	−4	4	−3	2	−1

numerical thermal models, it is observed that the influence on the heating process of the workpiece is rather low, as the compensation currents are relatively low, and most of their field lines are captured by the passive shield.

The active and passive shield together reduce the average B-field in the subdomain D to 1.34 μT (Table 1). This is about a factor 20 (26 dB) lower than the situation without any shielding.

The induced resistive heating in the workpiece W_{wp} is 1.097 kW, which means a slight decrease, compared to 1.133 kW in the unshielded case. There is a dissipation in the passive shield which equals about 10% of the heating in the workpiece. This could be lowered by decreasing the conductivity of the passive shield. Even a non-conductive passive shield can be useful: the optimal current in coil 9 of the active shield (Table 2) will then increase as the coil will have to carry the current that cannot flow in the passive shield any more. Due to the magnetic permeability of the passive shield, this compensation current of about 200 A (5% of the excitation current) will hardly influence the heating process. Moreover, the complex current in coil 9 will have a small imaginary part like the other eight currents of the active shield, while it is mainly imaginary in case of a conductive passive shield ($-5.03 + 66.58i$ A). In practice, all coils will be in series and only one current is provided (Section 4.4). In this case, only one compensation current and the number of turns of each coil can be chosen. If the numerical optimisation procedure results in nine currents with a similar phase, the nine optimal currents can be better approximated by one compensation current for all coils in series. Disadvantage of using a non-conductive passive shield is that the compensation currents up to 5% of the excitation current require a more expensive linear amplifier to generate them. Notice that with the conductive passive shield, the highest compensation current is only about 2% of the excitation current.

4.4. Passive and active shield with one independent current

The calculated field reduction with active and passive shielding can only be achieved in experiments in case the currents in the conductors are the nine independent calculated currents. Nine independent currents require nine expensive amplifiers. In practice, the nine coils will be in series and only one current will be provided to this ‘distributed’ coil by a current amplifier. Each of the nine coils will be constructed with a proper number of turns t_i, $i = 1 \ldots 9$. This number is estimated such that a good approximation of the best currents in Table 2 is obtained. Then, the least squares problem with 18 variables is rewritten for two variables—real and imaginary part of only one

compensation current—taking into account the number of turns of each coil. (8) is solved, but matrices A and C change to $A' = \mathrm{STAT}S^{\mathrm{T}}$ and $C' = \mathrm{STC}$, with

$$T = \begin{bmatrix} t_1 & 0 & 0 & 0 & \cdots & 0 \\ 0 & t_1 & 0 & 0 & \cdots & 0 \\ 0 & 0 & t_2 & 0 & \cdots & 0 \\ \vdots & \vdots & \vdots & \ddots & \vdots & \vdots \\ 0 & 0 & 0 & 0 & \cdots & t_9 \end{bmatrix} \quad \text{and} \quad S = \begin{bmatrix} 1 & 0 & 1 & \cdots & 0 \\ 0 & 1 & 0 & \cdots & 1 \end{bmatrix}. \tag{11}$$

This calculation is iterated with other numbers of turns. The numbers, providing the smallest cost, are kept and displayed in Table 2. A positive number means the orientation of the winding is the same as the orientation of the excitation coil.

For practical reasons, the numbers of turns should be chosen rather low. A good compromise between efficient field reduction and low numbers of turns is needed: in Table 2, there are in total 36 turns above and 36 below the $z = 0$ plane. Two of them are very close to the passive shield, 35 are above the operators head, and 35 below his feet. Each turn carries a current of 7.57–8.82i A. The resulting average B in the domain D is 2.18 μT. The reduction decreases from 26 dB in case of nine independent currents to 22 dB in case of 1 current.

5. Conclusions

Passive and active shields were added to an induction heater model, in order to reduce the stray field. The simulation takes into account some practical aspects related to the position of the passive and active shields and the currents in the active coils. To comply with the reference levels indicated by the international standards, the stray fields usually produced by induction heating equipment should be reduced up to 10 times (20 dB). Simulation results show that this reduction can be achieved with a small passive shield, and an active shield with one optimal current and two times nine coils.

Acknowledgements

This work was supported financially by GOA Project 99-200/4, by the FWO Project 39042099 and by the IUAP-Project P5/34 of the Belgian government. The second author is a postdoctoral researcher of FWO-Vlaanderen.

References

[1] G. Antonini, S. Cristina, An efficient digital controller for active shielding circuits, IEEE International Symposium on Electromagnetic Compatibility, 1, 21–25 August 2000, pp. 49–53.
[2] P. Girdinio, M. Nervi, Techniques for the automatic optimization of active shields, COMPEL 20 (2001) 732–739.
[3] ICNIRP-Guidelines. Guidelines for limiting exposure to time-varying electric, magnetic, and electromagnetic fields (up to 300 GHz), Health Phys. 74 (1998) 494–522.
[4] I. Mayergoyz, Nonlinear Diffusion of Electromagnetic Fields, Academic Press, London, 1998.
[5] R.B. Schulz, et al., Shielding theory and practice, IEEE Trans. Electromagnetic Compatibility 30 (1988) 187–201.